Application of a hybrid model for the numerical study of the generation of runaway electrons and the formation of high-pressure gas discharge

Application of a hybrid model for the numerical study of the generation of runaway electrons and the formation of high-pressure gas discharge

V.V. Lisenkov[1,2], Yu.I. Mamontov[2]

[1]Institute of Electrophysics UB RAS, 106 Amundsena St., Ekaterinburg, 620012, Russia
[2]Ural Federal University, 19 Mira St., Ekaterinburg, 620002, Russia

e-mail: lisenkov@iep.uran.ru

Abstract. The paper analyses the details of the application of the hybrid model for calculation of the formation of high-pressure gas discharge in conditions where the transition of electrons into runaway mode is possible. In hybrid model, PIC MC method is used only for calculation of runaway electrons, and the standard hydrodynamic approach is used for calculation of plasma electrons. Using such model can significantly reduce computing resources. The results of calculation of kinetics of electrons emitted from a micro-spike on the cathode during the formation of the cathode layer of nanosecond and sub-nanosecond high-pressure gas discharge are presented. The conditions of transition of electrons into runaway mode at this stage and their influence on the further formation of the gas discharge are analyzed.

1. Introduction

Nowadays, the generation of runaway electrons in high-pressure gases is one of the most studied topics in gas discharge physics. The most advanced method of modeling this process is the combination of the Monte Carlo method and the particle-in-cell method (PIC MC method). This method is realized, for example, in XOOPIC program package [1]. This package is based on the particle-in-cell method used to simulate the motion of charged particles under the action of external and self-electromagnetic fields. The electromagnetic field in this code is calculated using Maxwell's equations. The interaction of charged particles with gas is simulated by the Monte Carlo method (model of individual collisions). At each time step, one or another type of interaction (elastic scattering, excitation or ionization) is reproduced for the whole ensemble of particles with regard to their distribution functions, for which a random number generator and process cross-section database are employed. The package uses a 2D axially symmetric approximation. This code was successfully applied to solve the problem of the generation of a runaway electron beam in an atmospheric-pressure gas diode with a nonuniform electric field [2]. XOOPIC code was also applied for calculation of runaway electron generation in non-homogeneous high pressure gas containing high-temperature channel [3].

However, even in a two-dimensional formulation, this approach requires very large computational resources. This is explained by the fact that the numerical density of the runaway electrons is several orders of magnitude lower than the plasma (slow) electrons. Therefore, it is necessary to take into account a large number of particles. It is possible to significantly reduce computing resources in the

following way. PIC MC method is used only for calculation of runaway electrons, and the standard hydrodynamic method is used for calculation of plasma electrons. In paper [4], models using this approach are called as hybrid models. Paper [4] also contains references devoted to application of hybrid models.

The aim of present paper is the application of hybrid model to calculate the formation of high-pressure gas discharge with generation of runaway electrons.

2. Description of the model

The numerical model based on a system of balance equations for electrons, ions, and the Poisson's equation:

$$\frac{\partial n_e}{\partial t}+\frac{\partial n_e \mu_e E}{\partial x}=\nu_i(E)\,n_e+\int_{\varepsilon_{th}}^{\infty} \mathrm{v}\, n_{fe}(\varepsilon,x)\,\sigma_i(\varepsilon)\,d\varepsilon-\nu_{esc}(E)\,n_e-kr\,n_e n_i \tag{1}$$

$$\frac{\partial n_i}{\partial t}-\frac{\partial n_i \mu_i E}{\partial x}=\nu_i(E)\,n_e+\int_{\varepsilon_{th}}^{\infty} \mathrm{v}\, n_{fe}(\varepsilon,x)\,\sigma_i(\varepsilon)\,d\varepsilon-kr\,n_e n_i \tag{2}$$

$$\frac{\partial^2 \varphi}{\partial x^2}=\frac{e}{\varepsilon_o}(n_e-n_i) \tag{3}$$

where n_i, n_e, n_{fe} are the densities of ions, slow plasma electrons, and fast electrons, respectively; ν_i is the frequency of ionization by thermal and fast electrons, respectively; $\nu_{esc}=1/\tau_{esc}$, $\tau_{esc}(E)$ is the average time of the electron escape into the runaway mode; μ_e and μ_i are the electron and ion mobility, respectively; kr is the recombination coefficient; and ε_{th} is a conditional boundary between the slow plasma electrons and fast electrons..

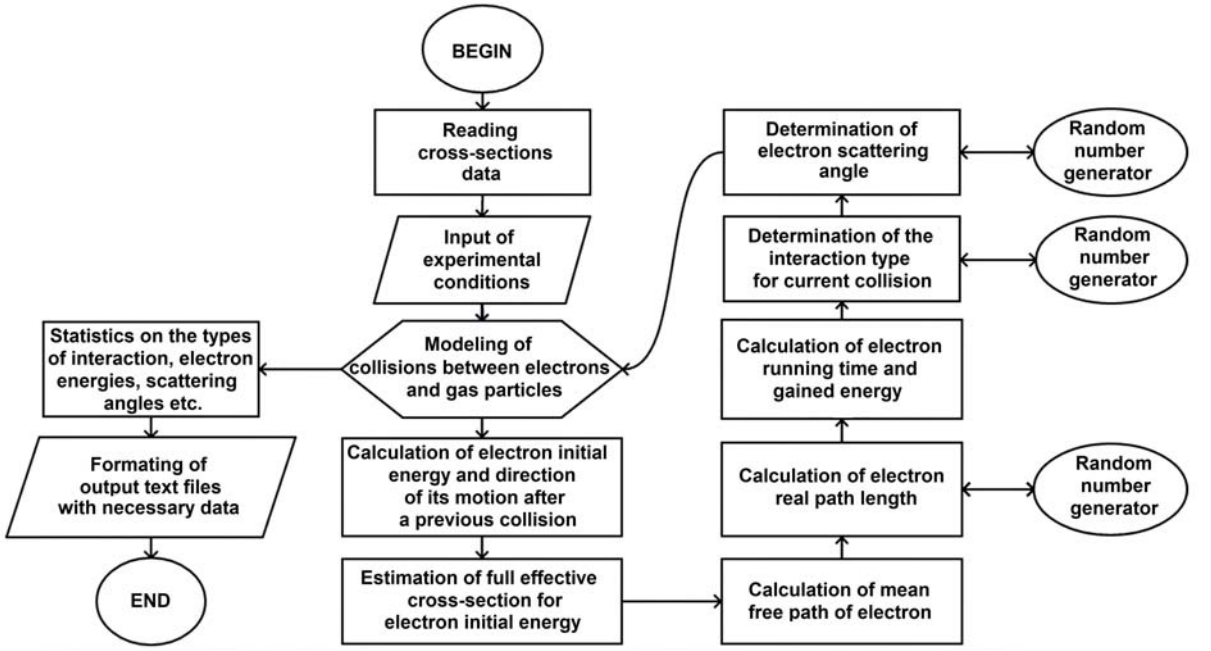

Figure 1. Block diagram of the Monte-Carlo module

Distribution of fast (runaway) electrons $n_{fe}(\varepsilon,x)$ as a function of energy and coordinate in the discharge gap was calculated by Monte-Carlo simulation of the electron motion. Field dependences of the kinetic coefficients including the probability of electron transition into the runaway mode were also obtained by Monte-Carlo simulation.

The block diagram of the Monte-Carlo software module is shown in Figure 1. The program took into account the gain of energy of the electron when it moves between collisions and losses as a result of inelastic collisions. The nature of the collision (elastic, excitation of the vibration or electronic levels, ionization) was played out with the help of a random number generator. The program was written by us in C++. The necessary data on cross sections were taken from [5-10]. The program was tested for different values of a uniform electric field. The obtained constants of ionization and drift velocity of the electron is well coincided with the data [10, 11].

3. Results of calculations

We have investigated the possibility of a runaway mode transition of an electron emitted from micro-spike on the cathode. The micro- spike was taken as a cone with height h and base $h/2$.

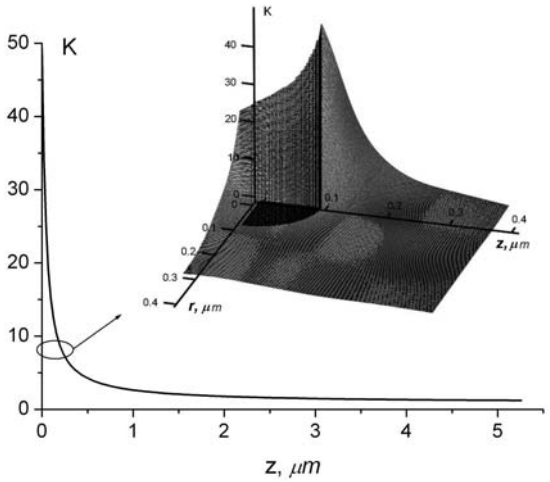

Figure 2. The distribution of the amplification factor of the electric field (K) for micro spike with f height (h) of 10 μm.

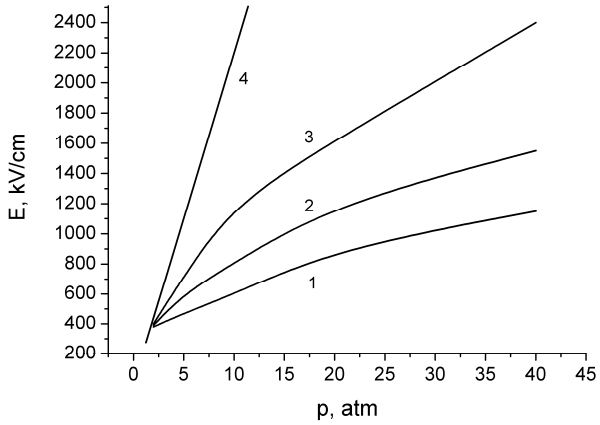

Figure 3. The dependence of the average strength of the electric field (E_m), which corresponds to the beginning of runaway mode, on the pressure (p).
1 – h = 20 μm; 2 – h = 10 μm; 3 – h = 5 μm;
4 – without micro-spike

To avoid singularities, the top of the cone was rounded with a hemisphere of radius 0.01 h. The presence of such a micro-spike on the flat surface of the cathode causes distortion of the electric field. The field near the top is significantly amplified in comparison with the average field value in the gap. In such cases, the the field amplification coefficient $K = E/E_m$ is usually used, where: E is the local value of the electric field, E_m is the average value of the field in the gap equal to $E_m = U/d$, where: U is the voltage on the gap, d is the cathode – anode distance (length of the gap). To calculate the spatial distribution of K, the Laplace equation was solved with ANSYS software package available in Ural Federal University [12]. Figure 2 shows the characteristic distribution of the electric field gain (K) of the micro-spike with h = 10 μm. The main graph shows the distribution of K along the axis of the cone (z). The top of the cone was taken as point of origin. The insertion shows the spatial distribution of K in the area of a sharp decline of E near the rounded top of the micro-spike. This top is shown as a dark area with K = 0 in the main graph.

Figure 3 shows the dependence of the average intensity of the electric field (E_m), at which the electrons emitted from the surface of the micro-spike escape to runaway mode, on the pressure (p). The curve 1 corresponds to the micro-spike with $h = 20$ μm, the curve 2 - $h = 10$ μm, the curve 3 - $h = 5$ μm, the straight line 4 corresponds to a uniform electric field (without micro-spike). For pressures less than 2 atm., all curves are almost identical. At higher pressures, the differences become more noticeable. In particular, for the pressure of 40 atm., micro-spike with $h = 20$ μm reduces the runaway threshold by 7 times, and micro-spike with $h = 10$ μm reduces by 5 times in comparison with the uniform field. This result is explained by the fact that in the case of micro-spike, the probability of runaway depends not only on specific, but on absolute value of the electric field intensity. Emitting from micro-spike electron appears in the region with sharply amplified electric the field (figure 2). Passing through this region almost without collisions the electron gains some energy. If this energy is large enough, it increases the probability of the electron escaping to runaway mode in non-amplified field in the gap.

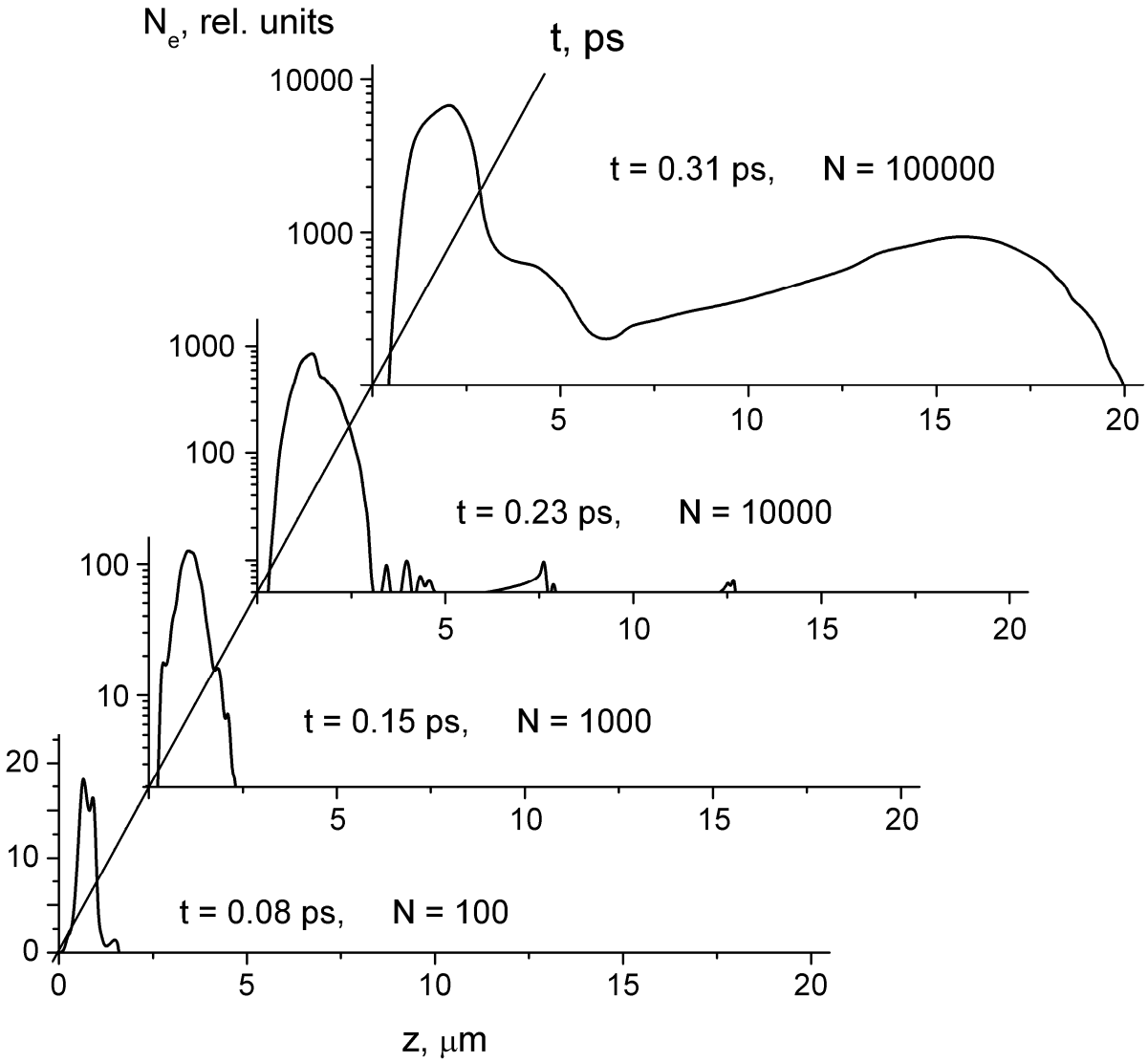

Figure 4. Evolution of space distribution of electrons in avalanche. N – number of electrons in avalanche. Beginning of time (t = 0) in this figure corresponds to t = 400 ps in figure 7.

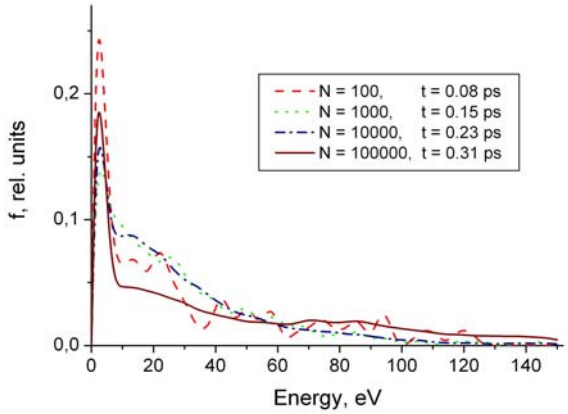

Figure 5. The evolution of electron energy distribution function. N – number of electrons in avalanche. Beginning of time (t = 0) in this figure corresponds to t = 400 ps in figure 7.

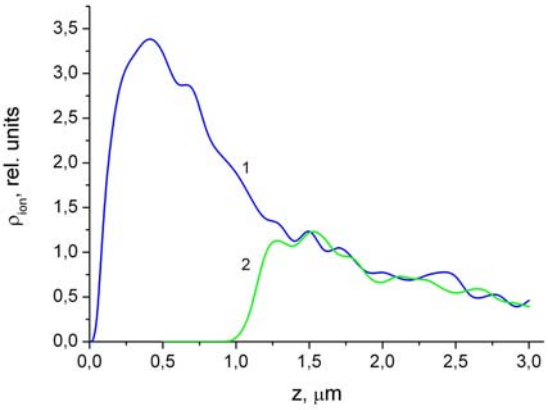

Figure 6. The dependence of the average ionization density on the distance for the electron emitted from the top of the micro-spike (curve 1), and appeared as a result of ionization at a distance of 0.5 μm (curve 2).

The program developed by us also allows simulating the development of an electronic avalanche. Figure 4 shows the evolution in time of the spatial distribution (*z*-coordinate distribution) of electrons in an avalanche in the amplified field of micro-spike with $h = 10$ μm at $E_m = 820$ kV/cm and $p = 10$ atm., which corresponds to the beginning of the runaway mode (figure 3). Figure 5 shows the time evolution of the electron energy distribution function in an avalanche under the same conditions. It is seen that with the increase in the number of electrons in the avalanche, the distribution function tends to a quasi-stationary state.

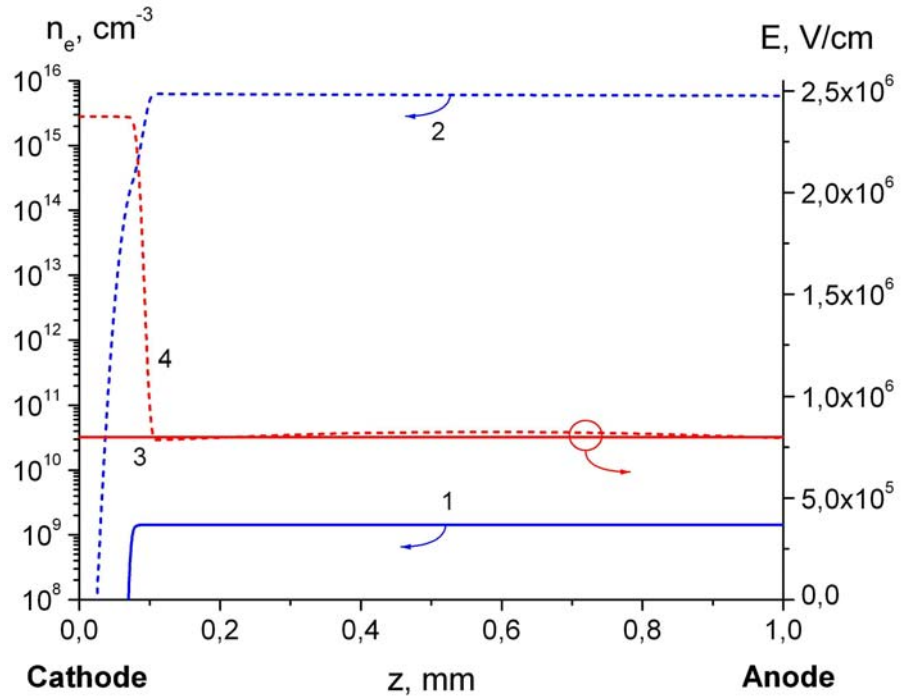

Figure 7. Space distribution of electron number density (1, 2) and electric field (3, 4) for different points of time. t = 400 ps (1, 3); t = 475 ps (2, 4).

This is also confirmed by figure 6, which shows the dependence of the average ionization density on the distance for the electron emitted from the top of the micro-spike (curve 1), and for the electron appeared as a result of ionization on a distance of 0.5 μm (curve 2). It is seen that, after a distance of ~10 μm, the behavior of the secondary electron is practically no different from the primary, which indicates the steady-state function of the electron energy distribution.

Figures 5 and 6 show a good statistics for the calculation of kinetic coefficients and using of hydrodynamic approach for plasma ("slow") electrons. This allows to apply the model presented at the beginning of present paper to calculate the formation of a high-pressure subnanosecond gas discharge. An example of such calculations is shown in figure 7. Nitrogen with a pressure of 10 atm. was used as a gas medium. The voltage pulse with an amplitude of 100 kV and a rise time of 500ps was applied to the gap with d = 1 mm. The results of calculations show that on the stage of formation of the cathode layer from the time of 400ps, it is possible for electrons to escape into runaway mode from the micro-spikes of different heights. By the time 475ps electrons can escape into runaway mode without micro-spikes on the cathode.

In our opinion, generated runaway electrons are able to initiate the development of instability in the forming cathode layer, which can subsequently lead to the contraction of discharge.

The work was supported by RFBR, Grant 16-08-00894.

References

[1] Verboncoeur J.P., Langdon A.B., Gladd N.T. 1995 *Comput. Phys. Commun*. **87** 199
[2] Shklyaev V.A., Belomyttsev S.Ya., and Ryzhov V.V. 2012 *J. Appl. Phys.* **112** 113303
[3] Lisenkov V.V., and Shklyaev V.A. 2015 *Physics of Plasmas* **22** 113507
[4] Levko D., Krasik Ya.E., Tarasenko V.F. 2012 *International Review of Physics* **6** 165
[5] Engelhardt A.G., Phelps A.V., Risk C.G. 1964 *Phys .Rev.* **135** A1566
[6] Schulz G.J. 1964 *Phys .Rev.* **135** A988-994
[7] Cartwright D.C. 1977 *Phys .Rev. A* **16** 1013
[8] Cartwright D.C. 1977 *Phys .Rev. A* **16** 1041
[9] Kieffer L.J., Dunn G.H. 1966 *Reviews of Modern Physics* **38** 1
[10] Phelps A.V., Pitchford L.C. 1985 *Phys .Rev. A* **31** 2932
[11] Jelenkovic B.M., Phelps A.V. 1987 *Phys .Rev. A* **36** 5310
[12] Ogorodnikova O.M. 2014 *Information technology of CAD/CAM/CAE* (2) 30